Demystifying Radio Astronomy

Krittika Summer Projects (KSP)

Niral Charan

Mentored by Atreyi Dasgupta and Mehul Goyal

Abstract

This report presents the topics in astronomy covered during the project. We covered some fundamental astronomy concepts then we moved on to the study of the basics of radiation physics. We aslo studied the structure of radio telescopes as well as their functioning. This was followed by using the Common Astronomy Software applications package for image detection. We aslo explored the use of Markov Chain Monte Carlo Methods to find the parameters of a model that fit given data. Overall we covered a wide range of topics in radio astronomy to get a good understanding of the techniques and tools used in this field. This work is part of the Kritikka Summer Projects (KSP) program.

Contents

1 Introductory Material **3**
- 1.1 Basic Introduction and History . . . 3
- 1.2 Basic Spectroscopy . . . 4
- 1.3 The Sky Coordinate System . . . 5
  - 1.3.1 Units or RA and DEC . . . 5
  - 1.3.2 Observer Centric Coordinates . . . 6
- 1.4 Appearent Sizes . . . 7
- 1.5 Radio Maps . . . 7
- 1.6 Activity: Radio Maps of Galaxies . . . 7
  - 1.6.1 M87 . . . 8
  - 1.6.2 Hydra A . . . 8
- 1.7 Activity: Jet Afterglow of GW170817 . . . 9

2 Radiation Physics **10**
- 2.1 Measures of Amount of Radiation . . . 10
  - 2.1.1 Total Energy Emitted . . . 10
  - 2.1.2 Luminosity . . . 10
  - 2.1.3 Flux . . . 10
  - 2.1.4 Flux Density . . . 11
  - 2.1.5 Intensity . . . 11
- 2.2 Blackbody Radiation . . . 11
  - 2.2.1 Wein's and Stefan-Boltzman Law . . . 12
  - 2.2.2 Rayleigh Jeans Approximation . . . 12
  - 2.2.3 Brightness Temperature . . . 12
- 2.3 Coherent Radiation . . . 12
- 2.4 Interference of Light . . . 13
- 2.5 Polarization . . . 13
- 2.6 The 21cm Line . . . 13
- 2.7 Activity: Plotting the CMB Spectrum . . . 14
- 2.8 Activity: Plotting the Galactic Rotation curve using the 21cm line . . . 15

3 Radio Telescopes **17**
- 3.1 Reflectors, Antennas and Feeds . . . 17
  - 3.1.1 Primary Reflectors . . . 18
- 3.2 Beam Pattern . . . 19
- 3.3 Feed Horn . . . 19
- 3.4 Surface Errors . . . 20

3.5 Gain, Noise, Noise Temperature . . . 20

4 CASA **21**
4.1 UV Data plots . . . 22
4.2 Imaging . . . 23
4.3 Side Effects of Calibration and Flagging . . . 24
4.4 Imaging the continuum of TW Hydra . . . 25

5 MCMC Methods **26**
5.1 Metropolis Hastings Algorithm . . . 26
5.2 Fitting a Model to the Jet Afterglow Light Curve of GW170817 . . . 27
5.2.1 Aquiring the data . . . 27
5.2.2 Dimensionality and Walkers . . . 28
5.2.3 Prior . . . 28
5.2.4 Likelihood . . . 28
5.2.5 Results . . . 28
5.3 Theoretical Explaination of the Phenomena . . . 29
5.3.1 Kilonova . . . 30
5.3.2 Jet Afterglow . . . 30

Bibliography **31**

Chapter 1

Introductory Material

1.1 Basic Introduction and History

Radio Astronomy is the subfield of astronomy that studies observations made in the radio frequencies of the electromagnetic spectrum. Its development in the mid-twentieth century opened up a new window on the universe. Before radio astronomy, astronomical observations were limited to the optical range.

Radio astronomy allows us to study objects that do not have significant radiation in the optical frequencies. For exmaple it allows us to study the cold interstellar medium as well as the cosmic microwave background radiation (In both cases temperature is too low for significant thermal radiation in the optical range). There is also a kind of non-thermal radiation called synchrotron emission which is prominent in the radio range. Synchrotron emission allows us to study interesting astronomical objects such as supernova remnants or kilonova remnants (which we will see more of later). Radio also has the somewhat practical significance of being mostly transparent to the Earth's atmosphere. Hence the largest radio telescopes are on the surface of the earth.

The history of radio astronomy truly starts with Karl Jansky of bell labs who was the first one to sucessfully detect astronomical radio emission. After Jansky it was grote Reber who mapped out the radio sky in further detail. With the advancement of radio technology post world war 2, more detailed maps were made. The next great leap in radio astronomy came with the discovery and subsequent detection of the 21cm line (which we will see more of as well). It can be used to map the distribution of hydrogen as well as find relative velocities.

The subsequent developments in radio astronomy were on two fronts. On the theoretical and discovery based front there were the discoveries of quasars, pulsars as well as the cosmic microwave background radiation. On the practical front the development of Radio telescopes that can use more than one antenna, at a large distance and combine their results greatly increaced our ability to make observations in the radio range.

1.2 Basic Spectroscopy

A plot that displays amount of radiation vs frequency or wavelength is called a spectrum. The spectrum of a source can lead us to a lot of information about its nature. Earlier the spectrum of a source was acheived using a dispersing device which shows different lines for different wavelengths. Spectral lines are lines that are of especially enhanced or reduced intensity. For radio telescopes the frequency seperation is done using electronic methods.

Spectra can be broadly classified into three types. They are

1. Continuous spectra: When a radiation source emits at all frequencies over a range without breaks, the spectrum is called a continuous spectrum and the emitting object is called a continuum source.

2. Bright line or emission line spectra: When a radiating object emits radiation onlyat some very specific frequencies, or wavelengths, the spectrum contains a set ofdiscrete bright lines. These lines of light are called emission lines. The reason that alight source would emit only at some very specific frequencies is due to the quantum physics of atomic and molecular structures. Basically the lines emitted correspond to some quantum state change.

3. Dark line or absorption line spectra: A more complicated and interesting case arises when the radiation from an intense continuum source passes through a cool, trans- parent gas of atoms or molecules. Some of the atoms or molecules in the gas can absorb photons from the continuum to raise them into a higher allowed energy level. The photons that they absorb must have exactly the same amount of energy that the atom or molecule gains, and so only the photons of certain, specific frequencies will be removed from the continuum. To an observer stationed beyond the cool gas, the spectrum will show the continuous spectrum of the background source with the radiation at these specific frequencies appearing darkened, thus the dark line nomen- clature. In a plot of intensity versus frequency, they will appear as dips or decreased intensity

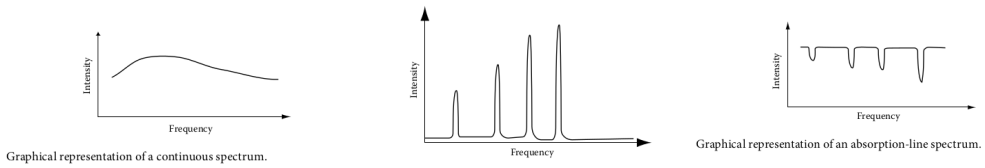

Figure 1.1: Continuous, Emissiona and Absorption Spectra

1.3 The Sky Coordinate System

The sky coordinate system describes an object int he sky using two coordinates. These are Right Ascension and Declination.

Right Ascension is the celestial equivalent of longitude. It is measured in hours, minutes and seconds. It is measured eastwards along the celestial equator from the vernal equinox. The vernal equinox is the point where the sun crosses the celestial equator from the southern hemisphere to the northern hemisphere. It is the point where the sun is at the start of spring.

Declination is the celestial equivalent of latitude. It is the angle between the object and the equatorial plane measured in degrees. Positive when the object is north of the celestial equator and negative when the object is south of the celestial equator.

The diagram makes the concept clear.

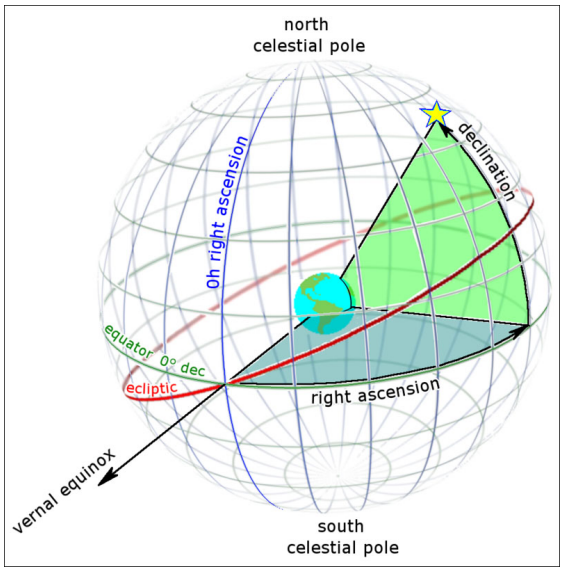

Figure 1.2: Sky Coordinate System

1.3.1 Units or RA and DEC

Declination is measured in degrees and that is self explanatory. Right ascension is usually expressed in units of time because it is more convinient that way. The reason for the time units is that the earth rotates 360 degrees in 24 hours. Using this conversion factor we get

$$1 \text{ hour } = \frac{360}{24} = 15 \text{ degrees} \tag{1.1}$$

1.3.2 Observer Centric Coordinates

Another way of describing an object is with respect to the observer. Here are some of the common terms used in this context along with their definitions.

- Horizon: This defines the limit of what parts of the sky you can see at any particular time.
- Zenith: The point in the sky directly above the observer. It changes continually as the observer rotates with the Earth except for the poles.
- Altitude: The angle between the object and the horizon. It is measured in degrees.
- Azimuth: The angle between the object and the north point on the horizon. It is measured in degrees.
- Meridian: The line that passes through the zenith and the north and south clestial poles.
- Transit: Means to pass through the meridian. Each object will pass through the meridian as the earth rotates.
- Hour angle: Amount of time in hours since the object transited. It is also the difference of the right ascension of the object and the right ascension of the meridian.
- Local sidereal time: The right ascension of the meridian.
- Universal Time: The time at the prime meridian (Greenwich Mean Time)

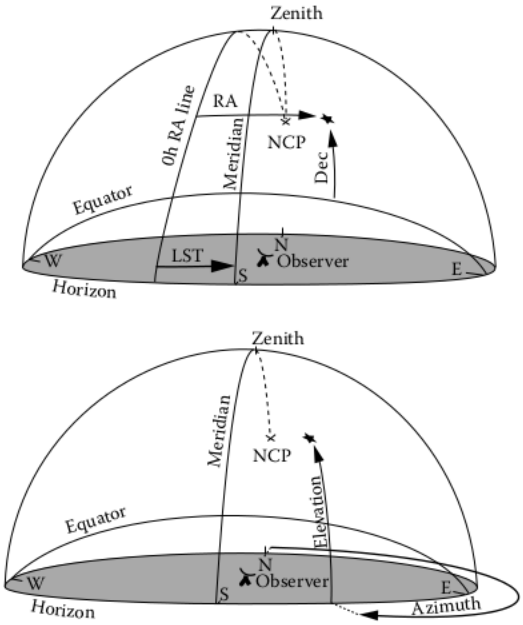

Figure 1.3: Observer-Centered Definitions

1.4 Appearent Sizes

Here we have two units that are useful. Radians for angles and Steradians for solid angles. At large distances (radii). The angle subtended by an object at distance r and whose length is l is given by:

$$\theta = \frac{s}{r} \approx \frac{l}{r}$$

The solid angle if an object has cross sectional area A is approximately:

$$\Omega = \frac{A}{r^2}$$

Also if a circular object subtends angle θ at the observer then the solid angle is:

$$\Omega = \theta^2 \frac{\pi}{4}$$

1.5 Radio Maps

To display a rdaio image in 2D we can use a few methods. The most simple is just to show the contours i.e lines of constant intensity. Another is a greyscale map that shows higher intensity regions as darker. Instead of greyscale we can also use custom colourmaps of our own choosing. The maps we have used for the galaxies are custom colourmaps.

1.6 Activity: Radio Maps of Galaxies

Our first activity was plotting the radio maps of two galaxies and comparing them to the optical as well as IR images. The objects I picked were Hydra A galaxy cluster and M49 elliptical galaxy. The images show clearly how astronomical objects can look different in different wavelength regions and also it shows how radio maps can reveal structures that are not visible in the optical range. This was great initial motivation towards the importance of radio astronomy.

1.6.1 M87

M87 is an elliptical galaxy which is also a strong radio source. We can see hat the radio data is significantly more elongated than the optical or IR data.

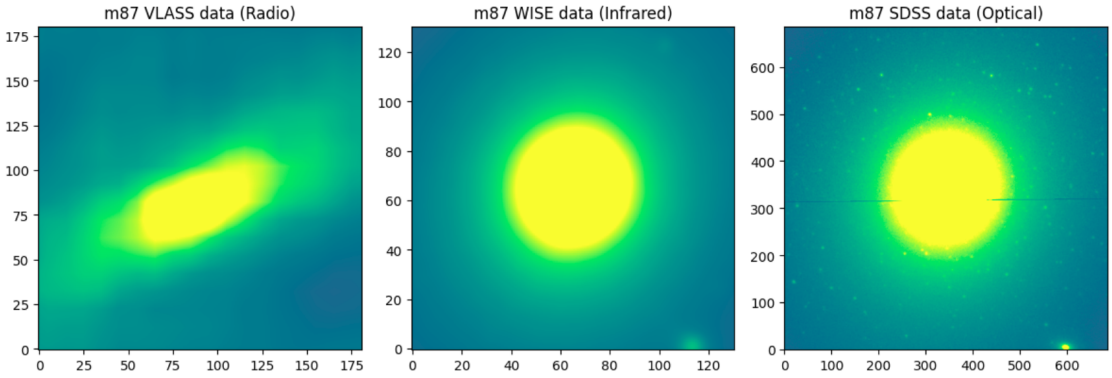

Figure 1.4: M87 in Radio, Optical and IR

1.6.2 Hydra A

Hydra A is a galaxy cluster. The radio data shows structures that are invisible in IR and optical data. Most prominent are the jets that are visible in the radio data. They are emitted by the central supermassive black hole.

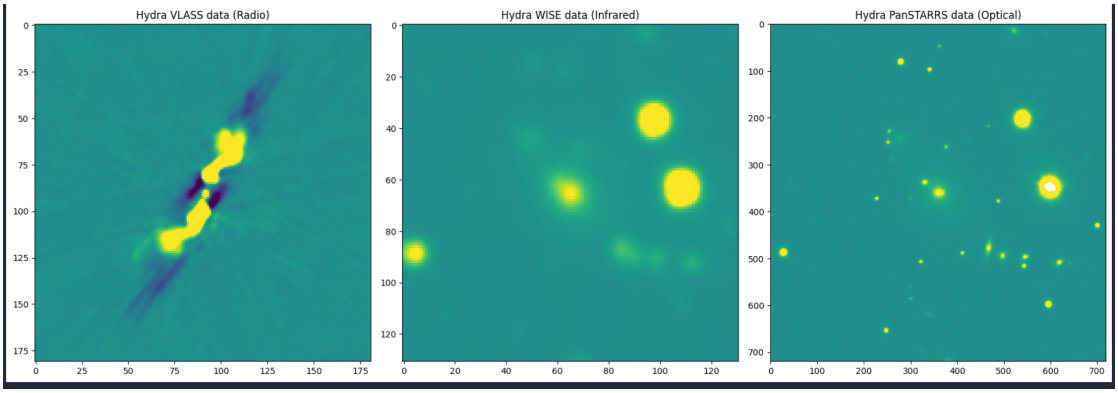

Figure 1.5: Hydra A in Radio, Optical and IR

1.7 Activity: Jet Afterglow of GW170817

GW170817 refers to the gravitational waves detected in 2017. It was the first detection of gravitational waves from a neutron star merger. It was also the first astronomical even that was studied in both gravitational waves and EM waves. The Gravitational waves were followed almost immidietly by a gamma ray burst. After that there was detection of thermal radiation from the kilonova (the merger remnant that spread out). After that we detected the afterglow of the jet that was emitted by the merger. We will be studying this in detail later on.

Here we have compiled the flux density vs time data for two different wavelengths, after appropriate scaling it shows remarkable structure. The blue points are in 3GHz radio range while the orange points are from X-ray observations.

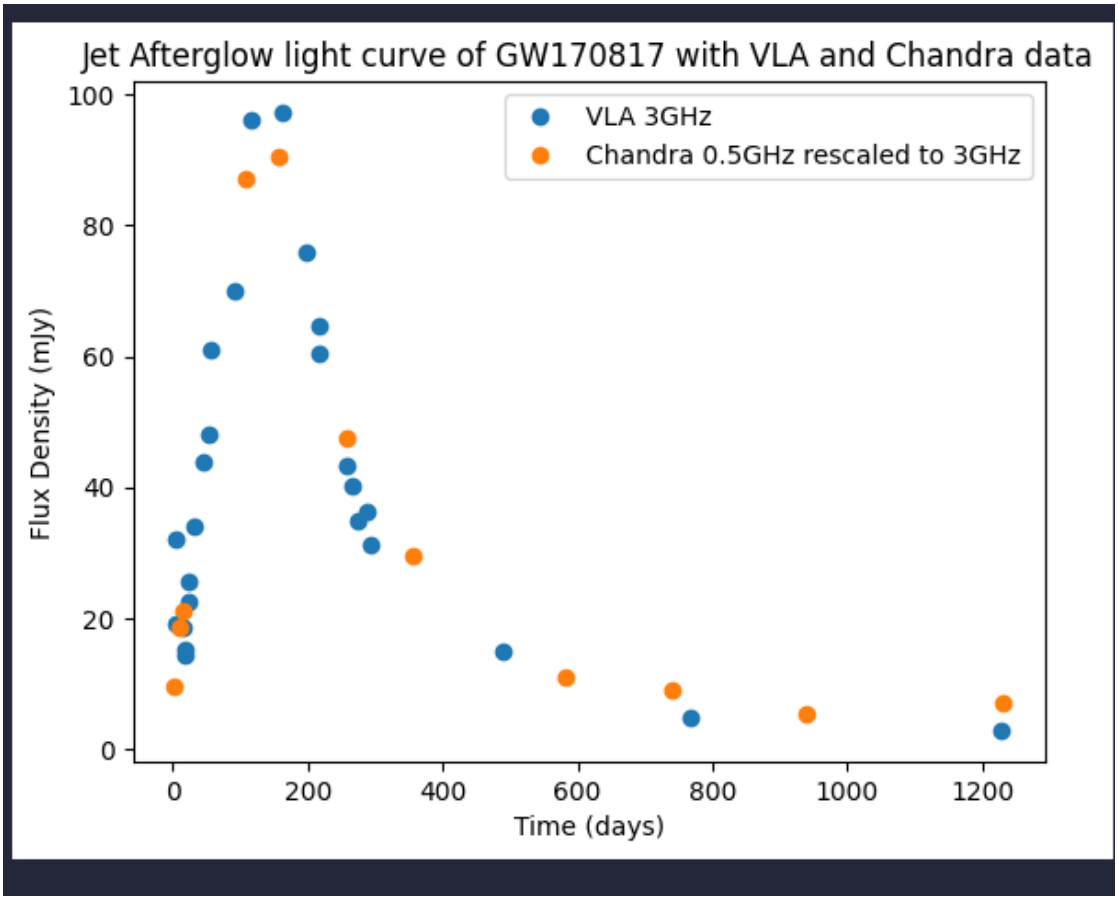

Figure 1.6: Jet Afterglow of GW170817

Later on we will fit the above data to a broken power law model.

Chapter 2

Radiation Physics

In order to analyze and interpret radiation we need to have an understanding of radiation physics and the various measures of amount of radiation that are used as well as their units.

2.1 Measures of Amount of Radiation

We begin by describing measures of amount of radiation emitted. These can broadly be thought of as belonging to three camps: Easy to understand Conceptually, Useful astronomically i.e reveal some information about the source and measurable directly.

2.1.1 Total Energy Emitted

One could describe a source in terms of total energy emitted over its entire lifetime over all frequencies. Clearly this not possible to measure. So we will have to at least normalize over time to get our next measurement.

2.1.2 Luminosity

Luminosity or power is the rate at which energy is emitted by a source. It can be calculated by dividing energy emitted by time. Again this is not something that can be measured since not all radiation from the source reaches us.

2.1.3 Flux

Flux is the radiation received by our telescope normalized wrt area. i.e It is Energy received by telescope per unit area. Another formula for it is the following in terms of luminosity (L).

$$F = \frac{L}{4\pi d^2}$$

Again this cannot be measured truly since we cannot measure radiation over the entire EM spectrum.

2.1.4 Flux Density

Flux density per unit frequency is the flux divided by the width in frequency of the observation. (It may also be per unit wavelength more common in optical cases)

$$F_v = \frac{F}{\Delta\nu}$$

From this we can derive

$$F = \int F_v d\nu$$

$$P = A_{eff} F$$

Finally this is a quantity that can be measured directly

2.1.5 Intensity

Intensity or specific brightness or just brightness is the flux density per unit solid angle. It is quite a fundamental quantity. Particularly useful since it is independent of distance. It is a direct measure of the brightness right at the surface of an object and hence reveals important information about said object. It is also directly linked to EM wave amplitude.

$$I_v = \frac{F_v}{\Omega}$$

$$I_v \propto E_0^2$$

2.2 Blackbody Radiation

A blackbody is an object that absorbs all radiation that falls on it. It also emits radiation at all frequencies. The radiation emitted by a blackbody is called blackbody radiation. Its spectrum depends only on the temperature of the body. In astronomy it is a good approximation for many objects and the spectral analysis allows us to determine the temperature of the object.

The theory of blackbody radiation was given by plank and it was one of the earlier sucesses of quantum mechanics. The spectrum of blackbody radiation is given by the Plank function. A basic way to think about is to think of almost a thermal distribution of photons. The Plank function is given as follows:

$$B_\nu(T) = \frac{2h\nu^3}{c^2} \frac{1}{e^{\frac{h\nu}{kT}} - 1}$$

Note that the conversion between frequency and wavelength functions is given by:

$$I_\lambda = \frac{c}{\lambda^2} I_\nu$$

Here is a plot of the Plank function for different temperatures. Notice the almost linear nature at lower temperatures. Note that this is a logarithmic plot.

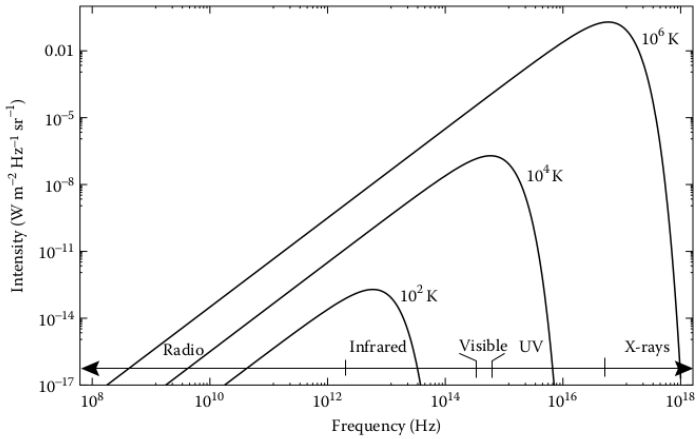

Figure 2.1: Plank Function for Different Temperatures

2.2.1 Wein's and Stefan-Boltzman Law

Wein's law is a simple relation between the temperature of a blackbody and the peak wavelength of its emission. It is given by:

$$\lambda T = 2.898 \times 10^{-3}$$

while Stefan Boltzman law states that the total energy emitted by a blackbody is proportional to the fourth power of its temperature.

2.2.2 Rayleigh Jeans Approximation

At most radio wavelengths we can approximate the plank function by a linear approximation. We can let the exponential term be linearly approximated using its Taylor series. From this we will get.:w

$$B_\nu(T) = \frac{2\nu^2 kT}{c^2}$$

2.2.3 Brightness Temperature

We can define a brightness temperature for a source. This is the temperature of a blackbody that would emit the same intensity as the source. For a source that is not a blackbody the brightness temperature can be lesser than the actual temperature of the source.

2.3 Coherent Radiation

When the radiation from two different sources is in phase then we say that the radiation is coherent radiation. Such radiation Has significantly higher intensity than incoherent radiation.

Mathematically if the phase difference between two sources is ϕ then the intensity of the combined radiation is given by:

$$I = I_1 + I_2 + 2\sqrt{I_1 I_2}\cos(\phi)$$

In particular for the coherent case and same intensity we get:

$$I = 4I_1$$

Hence the intensity is four times the intensity for a single source. In general for n sources the resultant intensity is n^2 times that of a single source. Interestingly this does not violate conservation of energy since the energy is distributed in a smaller solid angle.

2.4 Interference of Light

Interference is a phenomenon that occurs when two waves meet. In the classic example of youngs's double slit experiment for each point on the screen there is some path difference between the two waves which leads to a corresponding phase difference. The phase difference will influence the intensity of the light at that point. The phase difference caused by a path difference of d is given by:

$$\phi = \frac{2\pi d}{\lambda}$$

2.5 Polarization

Polarization is a property of light that describes the orientation of the electric field. Light can be linearly polarized, circularly polarized, elliptically or unpolarized. There are also Stokes parameters that describe the polarization of light.

2.6 The 21cm Line

The 21cm line is a spectral line emitted by neutral hydrogen corresponding to a transition between two hyperfine levels of the hydrogen atom. It is a very important line in radio astronomy since it allows us to map the distribution of hydrogen in the galaxy. It also allows us to measure relative velocities of objects. The line is redshifted or blueshifted depending on the relative velocity of the object. Shifted by the doppler formula the observed wavelength is given by:

$$\lambda = \lambda_0(1 + z)$$

Where z is given in terms of relative velocity approximately as $z = v/c$ One of our activities utilizes the 21cm line to measure the rotation curve of the galaxy.

2.7 Activity: Plotting the CMB Spectrum

The Cosmic Microwave Background radiation is the radiation left over from the big bang. It is very well approximated by a blackbody spectrum. We first plotted the CMB spectrum and then fit it to a blackbody spectrum. The fit was very good and the acheived temperature of $2.74K$ was very close to the accepted value of $2.726K$. Here is the fitted plot. For the fit we used the scipy library.

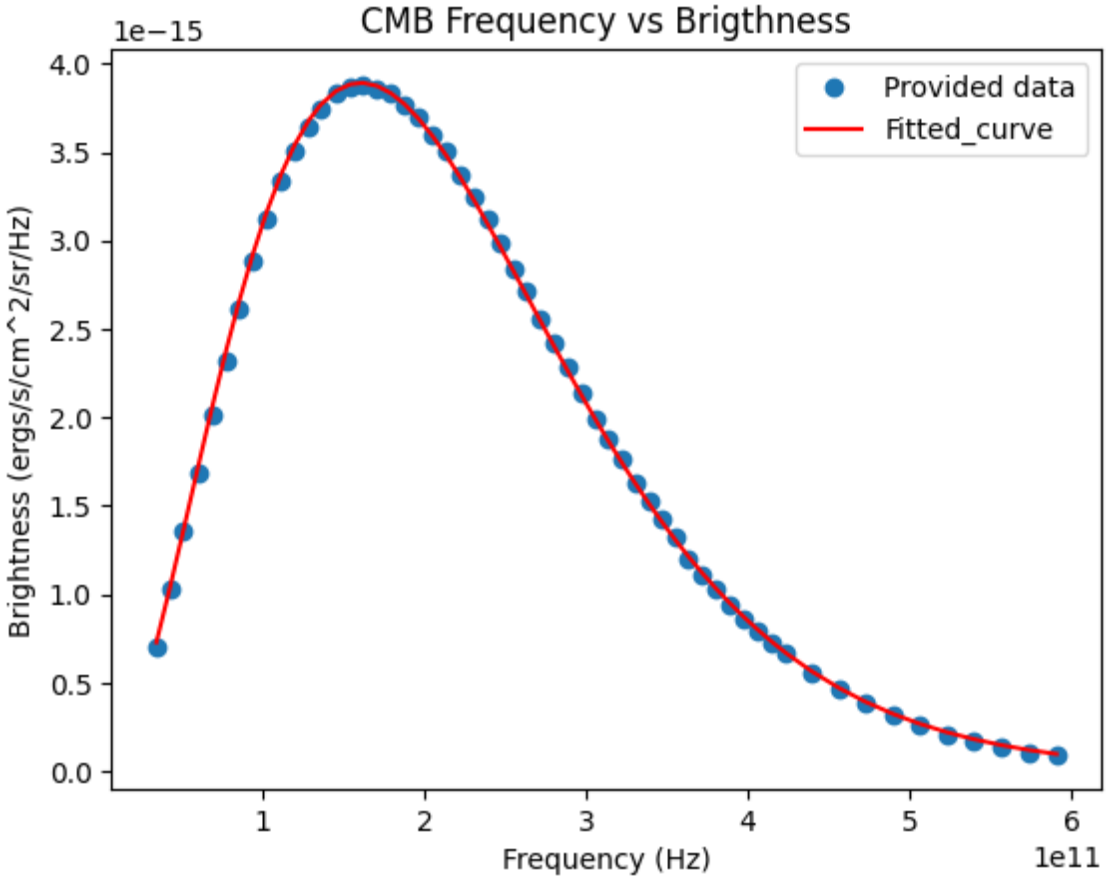

Figure 2.2: CMB Spectrum

2.8 Activity: Plotting the Galactic Rotation curve using the 21cm line

The 21cm line also allows us to measure the rotation curve of the galaxy. We were provided data of wavelength vs brightness in the 21cm region for different radial distances of the galaxy. For each radial distance we can calculate the velocity by first finding the observed wavelength (by fitting a gaussian) and then using the doppler formula. Here are some (not all) of the fitted gaussians as well as the rotation curve finally acheived.

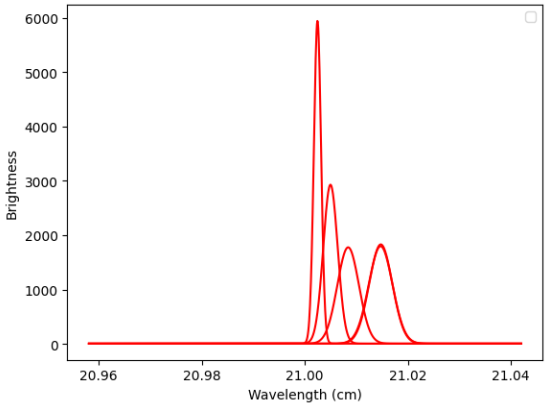

Figure 2.3: Rotation Curve of the Galaxy

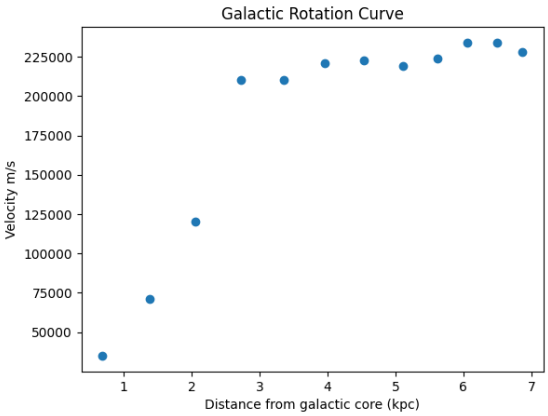

Figure 2.4: Rotation Curve of the Galaxy

We can see that the rotation curve is flat in the further regions. This cannot be explained by our current understanding of gravity and hence we have the concept of dark matter as one of the explainations for this. The other explaination is that gravity behaves differently at large scales. For a very rough explaination the velocity of an orbit at distance r is given by

$$v = \sqrt{\frac{GM}{r}}$$

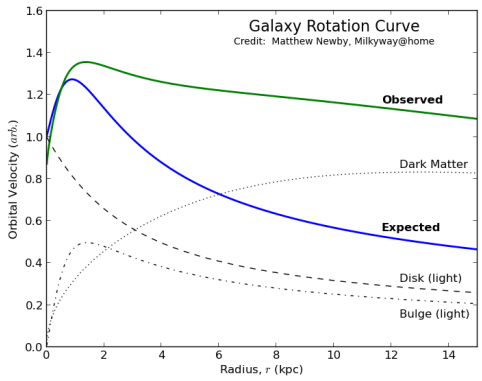

Figure 2.5: Expected vs Observed Rotation Curves

The initial almost linear region is where the density is somewhat constant hence $M \propto r^3$ and hence $v \propto r$. The flat region is where the density falls of sharply and hence we would expect $v \propto \sqrt{r}$ but instaed it remains constant. This is explained by some unseen mass that is present in the galaxy. The following diagram shows expected vs observed rotation curves. Notice how the one we have plotted matches the observed curves.

Chapter 3

Radio Telescopes

Radio telescopes allow us to observe the radio sky. A typical radio telescope consists of a primary reflector (or dish), feed, transmission line and receiver. Most radio telescopes are on an altitude azimuth mount and can point to any direction in the sky. The major aspect in which radio telescopes differ from optical ones is the maner in which light is detected. Radio photons are too low energy to be detected by semiconductor devices. Hence we must detect radio waves taking their wave nature into account.

Here is a schematic diagram of a radio telescope

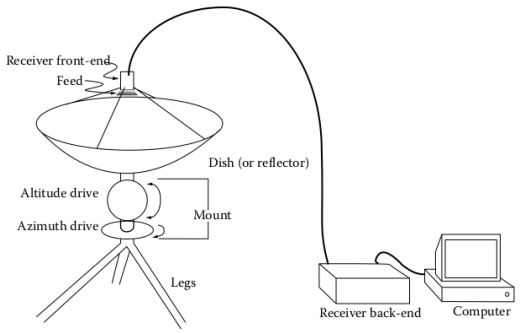

Figure 3.1: Radio Telescope

3.1 Reflectors, Antennas and Feeds

The antenna or reflector is the component of the telescope that collects the radiation. Precisely tough the antenna refers to the device that couples the elctromagnetic radiation to the transmission line. The reflector is the device that focuses the radiation. The antenna (or feed) is placed at the focus of the reflector. Usually a dipole antenns works for radio wavelengths.

3.1.1 Primary Reflectors

The Reflectors of most radio telescopes are parabolic in shape. Such a shape focuses all the incoming radiation to a single point. The size of the reflector determines the resolution of the telescope. At the focus usually a feed is kept. There can be a use of multiple feeds. A large primary reflector allows us to both see fainter objects as well as provides bettern angular range for observations. Note that the primary reflector must be opaque to radio waves usually it is not a solid surface but a mesh. Some telescopes also use a secondary reflector to focus the radiation to the feed. The ones where the feed is at the focus of the primary reflector are called prime focus telescopes. The ones where the feed is at the focus of the secondary reflector are called cassegrain telescopes. The cassegrain telescopes have the advantage of being able to place the feed at a more convenient location. The following diagram shows a primary and secondary reflector along with the feed.

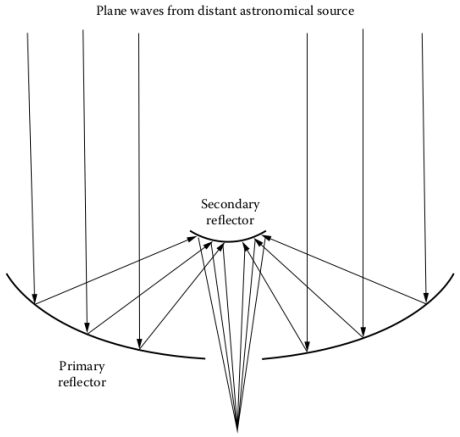

Figure 3.2: Primary and Secondary Reflector along with feed

3.2 Beam Pattern

Radio telescopes will be most sensitive to objects that are in the center of the beam. But they will still detect some of the radiation coming from off center beams, they will just be less sensitive towards them due to diffraction. The sensitivity vs angle curve is given below. The derivation of this curve is based on diffraction (It is the same as the curve we get from diffraction if you recall it from grade 12 physics) Due to this effect the resolution of a telescope is proportional to where

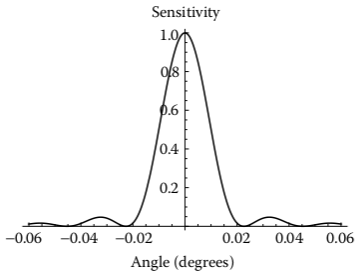

Figure 3.3: Beam Pattern

$$\frac{\lambda}{D}$$

D is the diameter of the telescope. Large radio telescope give smaller resolutiona llowing us to distinguish objects that are very close together

3.3 Feed Horn

In radio telescopes, antennas such as horn antennas couple electromagnetic (EM) waves from free space into transmission lines to send to receivers. Each feed horn, often flared, is connected to a receiver and operates efficiently within specific frequency ranges. These horns can be large, limiting the number of feeds that fit in a telescope's focal plane. Larger telescopes can have arrays of feeds, enabling simultaneous observations at multiple positions. The sensitivity and effectiveness of feed horns are influenced by their beam patterns and diffraction effects, which affect how radiation is collected and transmitted.

The beam pattern of a feed horn determines its illumination pattern on the primary reflector, influencing the telescope's performance. Ideally, the feed horn should uniformly illuminate the dish to maximize sensitivity but avoid detecting background radiation from beyond the dish. This balance is challenging to achieve, leading to either under-illumination or over-illumination. The edge taper, the ratio of sensitivity at the center of the reflector to its edge, describes this distribution. A larger feed horn provides a large edge taper, reducing sensitivity at the edges and minimizing spillover (radiation beyond the reflector). Conversely, a small edge taper enhances illumination efficiency but increases spillover.

The optimum edge taper, usually around 10 dB, strikes a balance between illumination efficiency and spillover, maximizing the telescope's effective collecting area. This taper also provides a good compromise between angular resolution and low sidelobe levels, with an angular resolution given by

$$\theta_{FWHM} = 1.15\lambda/D$$

. The resulting collecting area is about 82 percent of the reflector's physical area, though this doesn't account for physical blockages or imperfections in the reflector's shape.

3.4 Surface Errors

the primary reflector is never a perfect parabola. It always has some errors on the surface. If we charecterize a surface by the RMS deviation δz from the ideal surface. The rms phase error produced by the surface error is $4\pi\delta z/\lambda$.Then the effective loss in collecting area is given by Ruze equation as follows:

$$A_\delta = A_0 e^{-}(4\pi\delta z/\lambda)^2$$

If $\delta z/\lambda = 0.1$ then the telescope is said to have 1/10th wave accuracy.

3.5 Gain, Noise, Noise Temperature

Before final detection the signal is amplified through a series of amplifiers. The gain of a single amplifier is given by:

$$G = \frac{P_{out}}{P_{in}}$$

Each amplifier also adds noise to the signal. The noise can be modelled with respect to the equivalent noise temperature. The noise temperature of the amplifier is given by

$$T_{equiv} = \frac{P}{k\delta\nu}$$

Now we have a problem that subsequent amplifiers will amplify the noise as well. The total noise temperature of the system taking this into account is given by

$$T_n = T_1 + \frac{T_2}{G_1} + \frac{T_3}{G_1 G_2} \dots$$

where T_n is called the receiver noise temperature. The uncertainty in the measurement of power is given by the following:

$$\delta P = \frac{kT_n}{\sqrt{\delta\nu\tau}}$$

where τ is the integration time.

Chapter 4

CASA

The common astronomy software applications package, commonly known as CASA is a frequently used package to process data from radio telescopes. The data we used in this activity was from Atacama Large Millimeter/submillimeter Array (ALMA). We used the CASA package to process the image of the proto-planetary disk TW Hydra. We first did imaging of the disk and then did some basic analysis of the image.

4.1 UV Data plots

The UV data is the data that is collected by the telescope. It is the fourier transform of the image. Here is the data plotted for amplitude vs distance. The data can also be plotted on a scatter plot of U vs V

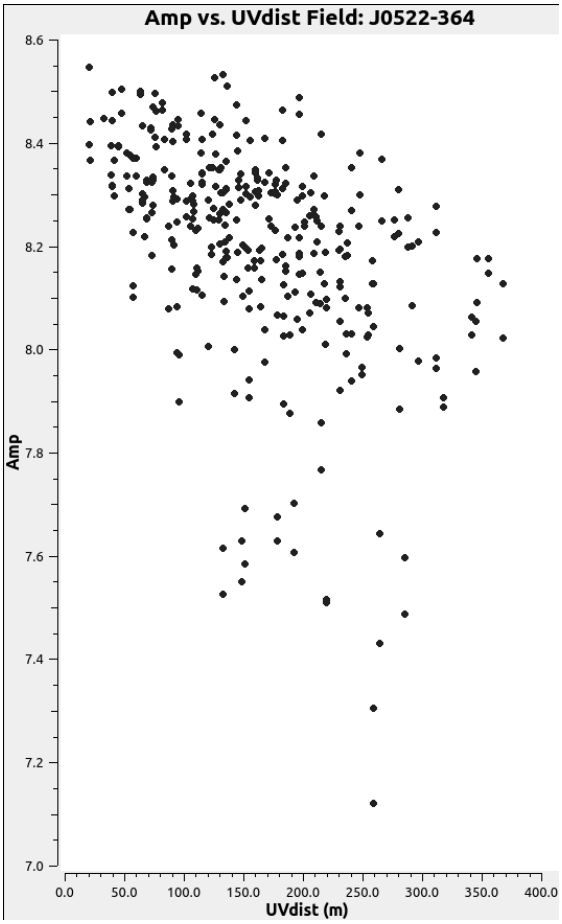

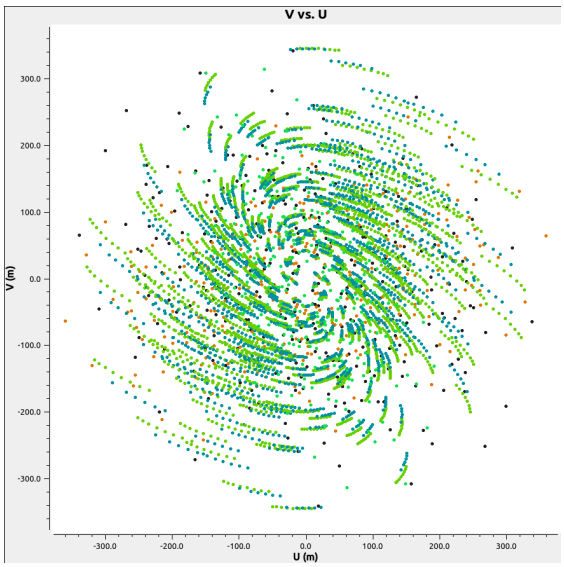

Figure 4.2: UV Dist

Figure 4.1: UV Data

4.2 Imaging

We image the data using tclean function from casa there are multiple options to tclean which can be tweaked in order to get an appropriate image. Here is the first image acheived by running tclean. We can also run the tclean function using briggs weighting to get another image. We can control the pixel size. here a large pixel size leads to a highly pixellated image

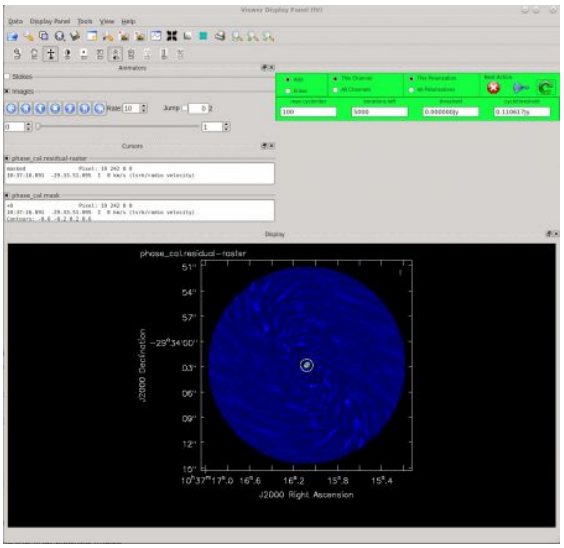

Figure 4.3: GUI after tclean showing clean mask (white oval)

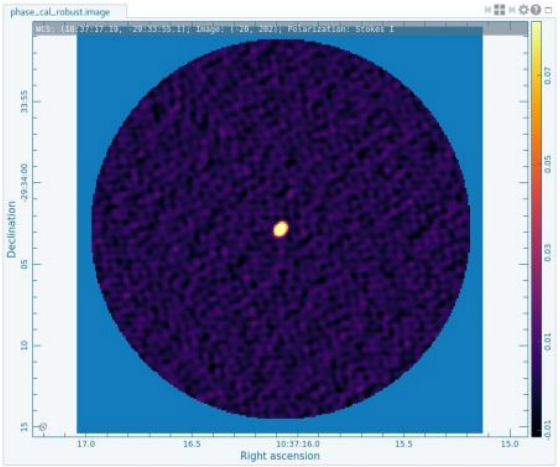

Figure 4.4: Image of the phase calibrator after tclean with briggs weighting.

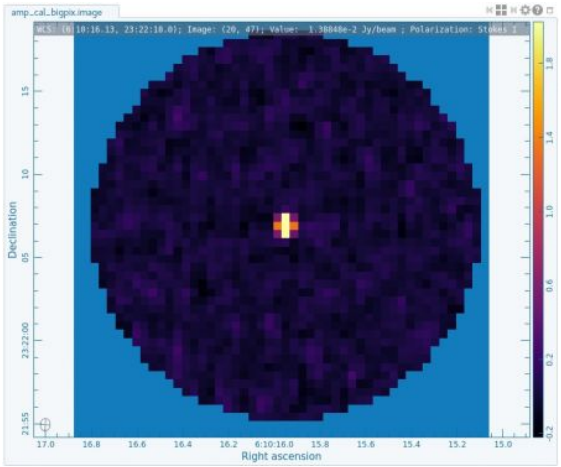

Figure 4.5: Image of the amplitude calibrator after tclean with a large pixel size

4.3 Side Effects of Calibration and Flagging

The data used above was all calibrated as well as bad data was flagged. Here we show the images that would be acheived without the above two procedures being done. The first image is acheived by using the phase calibrator without any calibration. The second image is that of the phase calibrator without any flagging of bad data[]

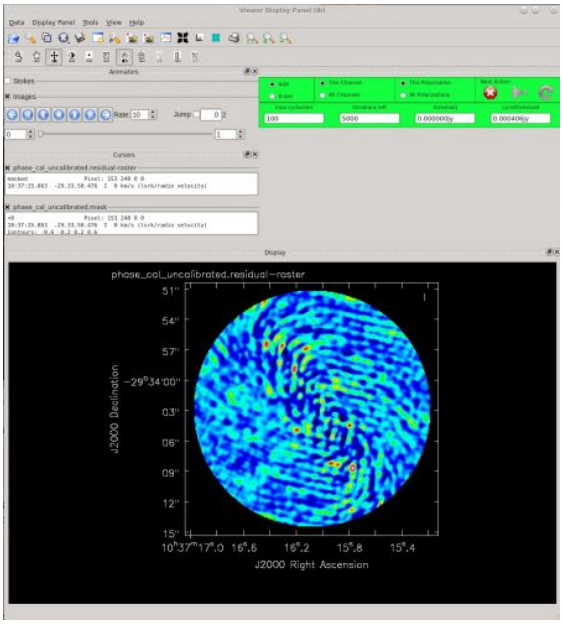

Figure 4.6: Phase Calibrator without any calibration

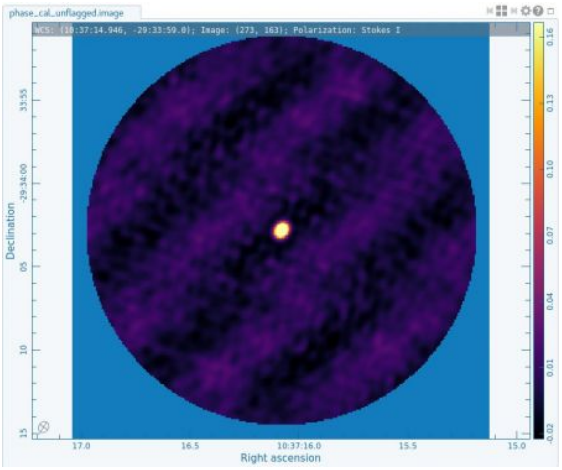

Figure 4.7: Image of the phase calibrator without flagging bad data

4.4 Imaging the continuum of TW Hydra

We finally imaged the continuum of TW hydra. This can be done in three ways mainly. We first began by smoothening the data out. Now we get the continuum image for TW Hydra. To get the proper image we will also need to correct for the primary beam of the individual dishes in the array. This can be done using the impbcor function. This correction needs to be applied before calculating values such as fluxes in the data.

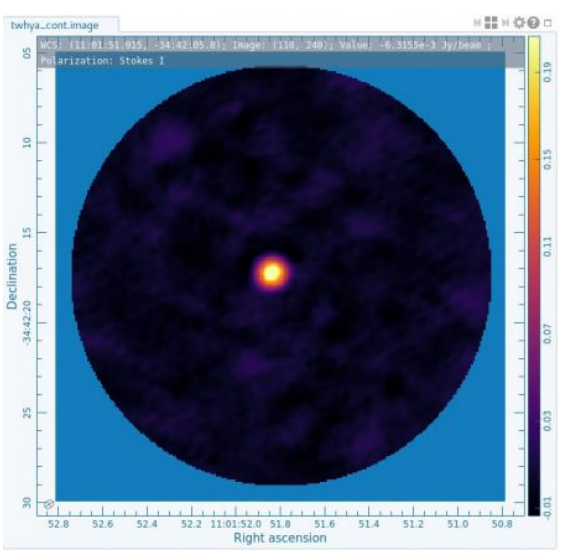

Figure 4.8: Continuum Image of TW Hydra

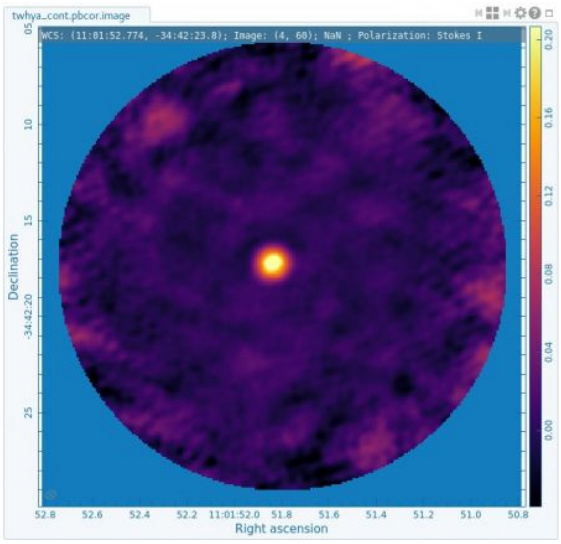

Figure 4.9: Continuum Image of TW Hydra with Primary Beam correction

Chapter 5

MCMC Methods

Markov Chain Monte Carlo methods (MCMC) methods are methods for sampling from a probability distribution. They are particularly useful when the distribution is high dimensional and we cannot sample from it directly. Or when we know the ratio of the distribution at two points but not the distribution itself. MCMC is useful if we want to sample from a distribution. For example if we want to fit a model to data, using MCMC we can find both the optimal parameters as well as the uncertainty in parameters along with other relationships of the parameters (using a corner plot).

5.1 Metropolis Hastings Algorithm

The simplest form of MCMC is the Metropolis Hastings algorithm. It is a method for sampling from a distribution. The algorithm requires the following inputs:

1. A function $f(\theta)$ that is proportional to the distribution we want to sample from.
2. A proposal distribution $q(\theta_t|\theta_{t-1})$ that gives the probability of moving from θ_{t-1} to θ_t. This is usually a gaussian distribution. It allows us to perform a random walk in parameter space.

After these inputs the algorithm is as follows:

1. Start at some initial point θ_0
2. For each iteration t:
   (a) Propose a new point θ_t from the proposal distribution.
   (b) Calculate the acceptance ratio $r = \frac{f(\theta_t)}{f(\theta_{t-1})}$
   (c) If $r > 1$ accept the new point.
   (d) If $r < 1$ accept the new point with probability r.
   (e) If the point is accepted set $\theta_t = \theta_t$ else set $\theta_t = \theta_{t-1}$

In essence the algorithm is performing a markovian random walk in parameter space. The frequency of each point in this chain finally converges to the stationary distribution of the chain which (by design) is the same as the distribution we want to sample from. In a Baysean statistical model the distribution we want to sample from is the posterior distribution of the parameters given the data. Hence $f(\theta)$ will be the prior $p(\theta)$ times the likelihood $p(D|\theta)$.

5.2 Fitting a Model to the Jet Afterglow Light Curve of GW170817

This was the final activity of the course. We took the jet afterglow lightcurve data of GW170817 from the paper written by Makathini et al. We then fit the data analytically to a broken power law model. We used the python library emcee to do the same.

The methedology to do so is described as follows:

5.2.1 Aquiring the data

The data was taken directly from the research paper. It is plotted in the following figure after proper rescaling (using β acquired by MCMC simulation). Please note that the plot is logarithmic. We also plotted the smoothened data with $\delta t/t = 1/15$.

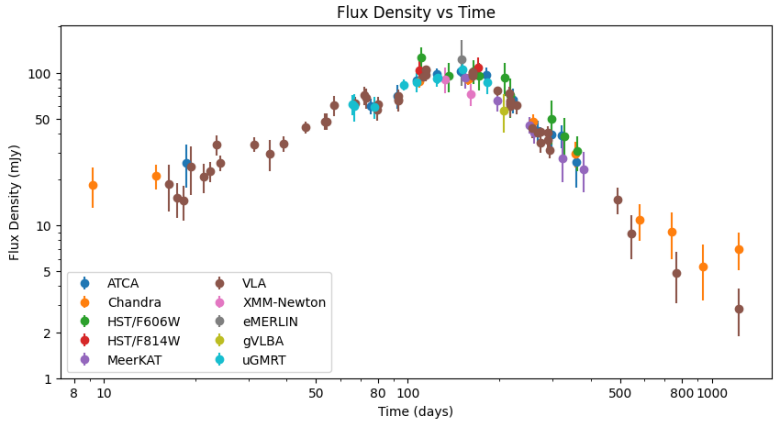

Figure 5.1: Jet Afterglow of GW170817

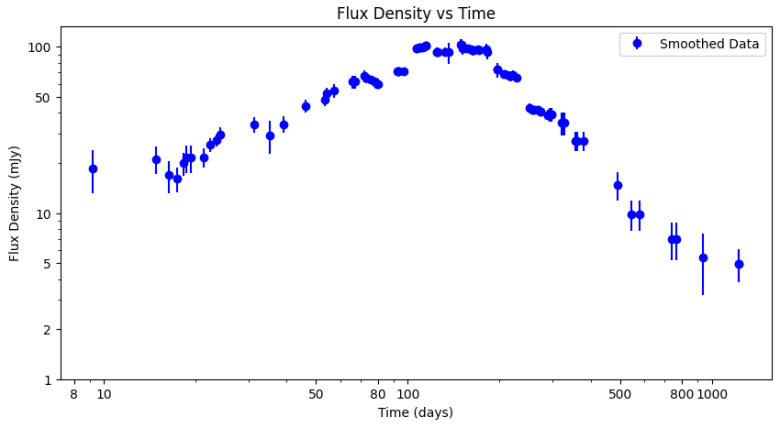

Figure 5.2: Jet Afterglow of GW170817

5.2.2 Dimensionality and Walkers

Since there are six variables in the model there are six dimensions. We use 50 walkers. They all begin with slightly different initial conditions and they also utilize parallelization in order to run the algorithm faster.

5.2.3 Prior

The prior incapsulates our knowledge of the parameters before we see the data. In our prior we just put reasonable physical bounds on all the parameters. Otherwise the prior used is uniform.

5.2.4 Likelihood

The likelihood used in our case is a simple chi squared likelihood. It is given formulaically as follows:

$$\chi^2 = -\frac{1}{2}\sum_i \frac{(y_i - f(x_i))^2}{\sigma_i^2}$$

Using the above formulas we ran the MCMC simulation. The results, after processing are as follows:

5.2.5 Results

The final corner plot of the parameters is as follows. It resembles the one in the paper quite well.

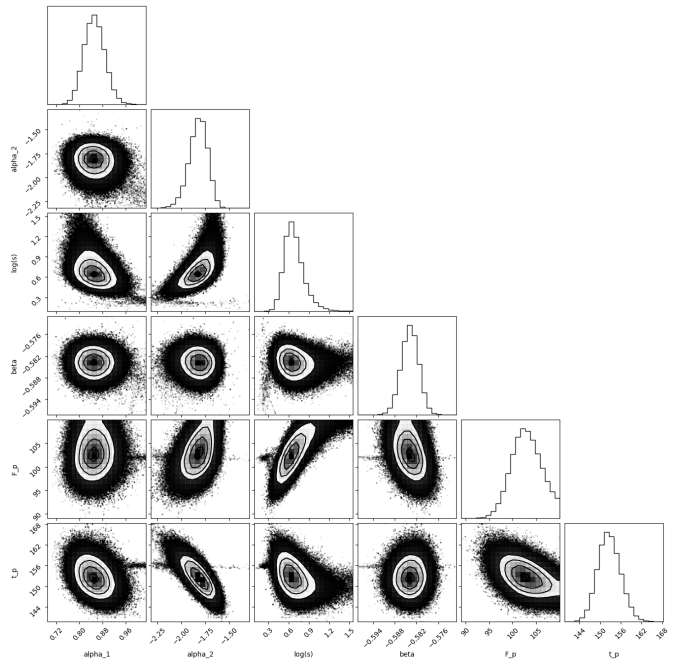

Figure 5.3: Corner Plot

A plot of the data along with the mean values acheived by the MCMC simulation is as follows: Finally here is a plot comparing the values acheived to those given in the paper. They are quite

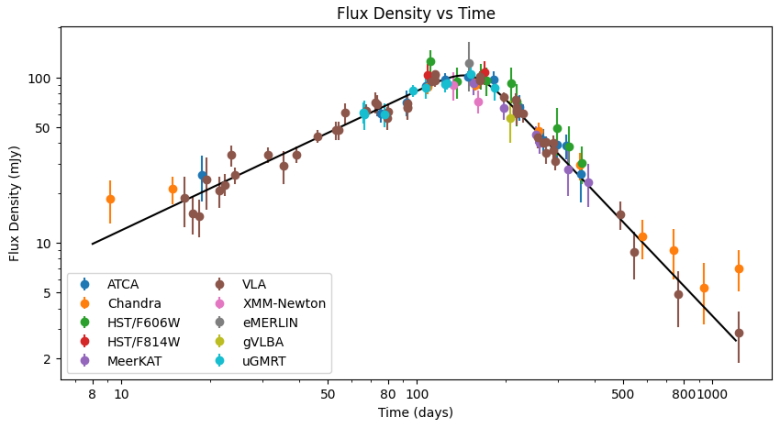

Figure 5.4: Fit to the Data

close.

Quantity	Value	Value (Paper)
α_1	0.852 ± 0.03	0.86 ± 0.04
α_2	-1.824 ± 0.09	-1.92 ± 0.12
$log(s)$	0.685 ± 0.154	0.56 ± 0.12
β	-0.584 ± 0.002	-0.584 ± 0.002
F_p	103 ± 3	101 ± 3
t_p	153 ± 3	155 ± 4

Figure 5.5: Comparison with Paper

5.3 Theoretical Explaination of the Phenomena

GW170817 was a neutron star merger whose gravitational waves were detected in August 2017. The gravitational waves were followed up by a gamma ray burst just 1.7 seconds after it. After this there was an observation of the kilonova produced by the merger. The kilonova was followed by the afterglow of the jet produced by the merger.

5.3.1 Kilonova

The kilonova refers to the ejected matter from the merger that spread out almost spherically. The observed radiation from the kilonova was thermal radiation. The analysis of the radiation allowed us to determine the mass of the ejected matter as well as the velocity of the matter. The radiation was also used to determine the composition of the ejected matter. The ejected matter was found to be rich in heavy elements. The kilonova was also used to determine the Hubble constant. It confirmed the theory that many of the heavier elements are produced in neutron star mergers.

5.3.2 Jet Afterglow

The radiation emmitted by the jet was synchrotron emission by the electrons travelling at very high speeds. The afterglow data suggested that we were not on the axis of the jet rather we were at some angle for it. In that case one would normally expect a smooth increace then smooth decreace at the same rate for the flux density ($\alpha_2 = -\alpha_1$). But this was not the case. This problem was explained by the fact that the jet also had cocoon like wings whose radiation makes the flux density higher in the earlier part of the observations. As the jet sped up the radiation increaced to a peak, then as it slowed down the radiation decreaced. This was the reason for the broken power law fit. The cocoon explained $\alpha_1 \neq \alpha_2$ and the jet explained the overall shape of the light curve.

A simulation of the jet afterglow that was done on physical parameters by the paper (as opposed to our analytical fit) was able to determine both the angle of the jet $\theta_j \approx 10^{-4}$ deg as well as the angle at which the jet was being viewed by us at around 35 deg. The following diagram better illustrates the discussion

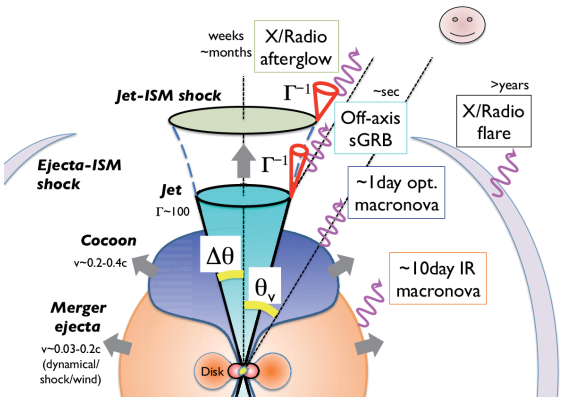

Bibliography

[CIR24] CIRADA. CIRADA Cutout Service, 2024.

[Kc24] Mooley Kunal and collaborators. GW170817 Afterglow Data, 2024.

[KHK20] John D. Kraus, Gerald M. Heiligman, and Timothy Koch. *Fundamentals of Radio Astronomy: Observational Methods*. CRC Press, Boca Raton, FL, 2nd edition, 2020.

[MCE+] J. C. Mather, E. S. Cheng, R. E. Eplee, Jr., R. Isaacman, R. A. Shafer, J. M. Weisberg, and E. L. Wright. A preliminary measurement of the Cosmic Microwave B ackground Spectrum by the Cosmic Background Explorer (COBE) Satellite.

[NAS24] NASA/GSFC. Flexible image transport system (FITS), 2024.

[NRA24] NRAO. First Look at Imaging CASA 6.4, 2024. Accessed: 2024-07-28.